A Time Domain Noncontact Fluorescence Tomography System for Breast Cancer Diagnosis

Guo Hui, Meng Wei, Wang Tingting, Li Jiao, Zhao Huijuan *, Gao Feng
College of Precision Instruments and Optoelectronics Engineering, Tianjin University, Tianjin, 300072, P. R. China
huijuanzhao@tju.edu.cn

ABSTRACT

A time domain noncontact fluorescence tomography system and the corresponding reconstruction algorithm towards the early diagnosis of breast cancer are developed. The time domain system based on the time-correlated single photon counting technique is adopted to provide both the high sensitivity in detection and good capability in multi-parameter reconstruction. Comparing to the conventional contact measurement mode, the noncontact system with light scanning can provide more measurement data for improving the spatial resolution of the images. The performance and efficacy of the system is evaluated with measurements on solid phantoms. For the phantom with single fluorescent target, the fluorescence yield and lifetime were simultaneously reconstructed with good quality. For the phantom with two fluorescent targets, the targets with the center-to-center separation of 20mm and the edge separation of 15mm can be distinguished. Measurements also show that the reconstructed yields are linear to the concentration of the fluorescence dye. The results demonstrated the potential of the system in the *in vivo* diagnosis of the early breast cancer.

Keywords: Fluorescence tomography; Breast cancer; Time domain; TCSPC; Noncontact

1 . INTRODUCTION

Compared with the current breast imaging methods such as mammography, ultrasonic imaging and nuclear magnetic resonance, diffuse optical tomography (DOT) has become one of the most promising breast imaging techniques due to its advantages of good specialty, sensitivity and safety[1]. Based on the technology of DOT, the fluorescence diffuse optical tomography (FDOT) introduces Indocyanine Green (ICG) as the fluorescence enhancement agent[2], which greatly improves the image contrast. FDOT relies on the presence of fluorophore molecules in tissue that re-radiate fluorescent light after illumination by the excitation light. Tumor-to-normal tissue contrast based on FDOT with the fluorophore Indocyanine Green was two-to-four-fold higher than contrast based on endogenous contrasts such as hemoglobin and scattering parameters obtained with traditional diffuse optical tomography. FDOT can reconstruct not only the yield but also the lifetime, which can improve the accuracy of the early cancer diagnosis. Since the fluorescence lifetime is independent on the concentration, photobleaching, and some other extrinsic factors but sensitive to the environmental information such as pH, viscosity and oxyhemoglobin saturation, thus it can provide functional information for the early cancer diagnosis[3].

Two types of measuring system that have been proven effective for simultaneously reconstructing both fluorescence

Multimodal Biomedical Imaging VII, edited by Fred S. Azar, Xavier Intes, Proc. of SPIE Vol. 8216, 82160Z · © 2012 SPIE · CCC code: 1605-7422/12/$18 · doi: 10.1117/12.907575

yield and lifetime are frequency domain and time domain systems[4]. The time domain system used in this paper utilizes the ultra-short pulse laser as the light source. Both the fluorescence yield and lifetime can be reconstructed through time resolved measurement of the transient overflow light from the tissue surface. More complete optical information can be provided to achieve higher resolution from time domain because of the measured information including various modulation frequencies. Currently, the time domain measurement technique is widely adopted in fluorescence tomography. One system using Gated Optical Intensifier coupled to the CCD as the detector is commonly available in small animal fluorescence molecular imaging field[5]. But for the breast-like bulk tissue imaging, the GOI-CCD system has several weaknesses in aspects of detection sensitivity and others. Another system employing Time-Correlated Single Photon Counting Techniques (TCSPC) is extensively applied to the time domain optical signal measurement for its high sensitivity[6]. This time domain measuring system based TCSPC techniques is used in this paper.

The conventional way of detection for the breast imaging requires the use of a number of detection fibers put in contact with the object. The fiber-based system have several limitations due to the limited number of fiber that can be practically used, which may leads to insufficient spatial sampling of photon signals[7]. Besides, the coupling issue between tissue and the optical fibers can not be avoided. To solve these problems, the noncontact scanning system is developed. For the simplification of mathematical model, the breast is compressed to confirm regular geometric boundary condition. The noncontact detection can provide the flexibility of large detector arrays, which improves the special resolution. Besides, ICG is introduced to improve the contrast of the target and background. Furthermore, the performance and efficacy of the developed system was evaluated by measurements on solid phantoms.

2. THE MASUREMENT SYSTEM

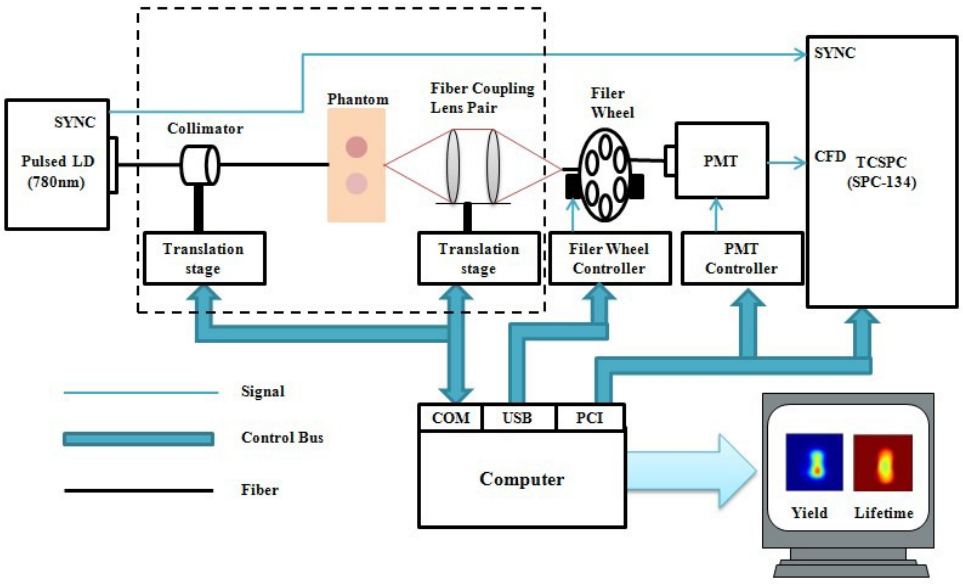

Figure 1 Schematic diagram of the fluorescence diffuse optical tomography system

Figure 1 shows the block diagram of the noncontact fluorescence tomography system. The measurement system is

composed of the single TCSPC measurement channel, the spatial light scanning device and the controlling software.

The TCSPC measurement channel is mainly composed of light source, photoelectric detector and single photon counting module. The light source (PDL828, SepiaII, PicoQuant) with the central wavelength of 780nm, the maximum repetition frequency of 80MHz and the FWHM less than 150ps was applied to illuminate the phantom. The emitted light was then transformed into electronic pulses by PMT (PMC-100-20, Becker&Hickl). The temporal profile, which measure the arrival distribution of photons as a function of time at different locations, are acquired through the time-correlated photon counting channel. A motor drove filter wheel (FW102B, Thorlabs) was placed before the PMT to filter the exiting light by a long pass filter (Semrock, BLP01) and an absorption filter. Besides, a fiber collimator was placed before the filter wheel to assure the performance of the filter.

The PMT+TCSPC based system is one of the most sensitive equipments for the low level light signal detection. The usable count rate of the single photon counting technology module SPC-14 (Becker&Hickl, Germany) employed in fluorescence measurement system in this paper is up to 20MHz. The photon counting technique, as a digital technique recording distributed photon pulses, can measure the light current intensity, which is weaker than the thermal noise (10^{-14}W) of photoelectric detector itself at room temperature. In photon counting state, the output electronic pulses number is proportional to the number of input photons. Therefore, the number of photons can be determined by counting the number of electronic pulses accordingly and the photon counting sensitivity depends on the integration time. To satisfy the bulk tissue imaging requirements, optical attenuators are installed in front of the system to increase the dynamic range.

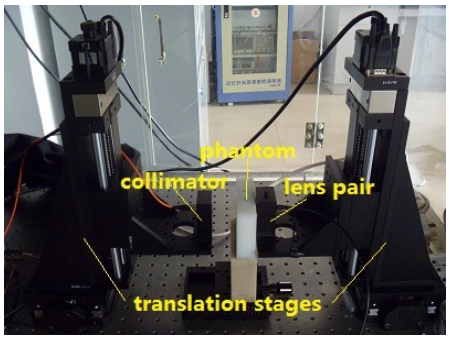

Figure 2 Photo of the scanning appliance

The block diagram of the spatial light scanning appliance is given in the dotted line box in Fig. 1 and Fig.2 shows the photo of the appliance. The appliance was developed based on the scanning pattern of mammography. For the clinical application, the breast is compressed and immersed into a fixed imaging chamber filled with an appropriate matching fluid composed of intralipid solution and india ink. For the realization of noncontact scanning measurement, the collimator lens (F230FC-B, Thorlabs) are employed to produce narrow collimated light beam being perpendicularly incident on the surface of imaging chamber. Meanwhile, the focusing lens pair is placed behind the imaging chamber to couple the emission light into detector fiber. The lens pair consists of two non-spherical coated lenses. The phantom-end lens with bigger numerical aperture NA=0.55 is conductive to collect as much light emitted from the phantom into the lens as possible. By using the fiber-end lens with numerical aperture NA=0.16, more light being incident into the lens can be coupled into detector fiber. The incident part and the detection part are positioned on the 2-D translation stages, respectively. X-axial translation stage and y-axial translation stage are controlled by computer to accomplish scanning both on the surface of illumination and measurement. The translation stages controlled by electric cabinet, which is

connected to computer by RS232 serial ports, can move freely with the resolution of 1.25μm along x axial direction and y axial direction.

The automatic control software was developed under the Windows platform by using Visual Studio 2008 to realize the functions such as the time-correlated single photon curve measurement, parameter settings and continuous scanning measurement.

3. RECONSTRUCTION ALGORITHM

The time domain fluorescence tomography is aimed to reconstruct the spatial distribution of fluorescence yield and lifetime based on the photon propagation model when the optical parameters of the background are known[8]. The forward model can be obtained by the time-domain coupled diffusion equations of the excited light and the fluorescence[9]. The fluorescence parameters are reconstructed with the algorithm based on a linear generalized pulse spectrum technique, which is certified effective in resolution of diffusion-based inverse problem[10].

The normalized Born-ratio model was applied to process the data in order to eliminate the uncertainty of time-origin and the impact of the systematic errors. Under the extrapolated boundary condition, the analytical solution of the diffuse equation for an infinite slab transmission optical model is employed as the forward model. The resultant linear inversions are solved using an algebraic reconstruction technique based on row operation. A pair of real transform factors is introduced to separate the fluorescent yield and lifetime[11]. The implementation procedure of image reconstruction algorithm is described below[12].

$$\begin{cases} \Phi_m\left(\mathbf{r_d},\mathbf{r_s},q\right)=\int_V cG_m\left(\mathbf{r_d},\mathbf{r},q\right)\Phi_x\left(\mathbf{r},\mathbf{r_s},q\right)x\left(\mathbf{r},q\right)dV \\ x\left(\mathbf{r},q\right)=\eta\mu_{af}\,/\left(1+q\tau\left(\mathbf{r}\right)\right) \end{cases} \tag{1}$$

where $\Phi_m\left(\mathbf{r_d},\mathbf{r_s},q\right)$ denotes the Laplace transformed fluorescence density when the source at position $\mathbf{r_s}$ and the detection at position $\mathbf{r_d}$, $G_m\left(\mathbf{r_d},\mathbf{r_s},q\right)$ denotes the Laplace transformed Green function when the source at position $\mathbf{r}$ and the detection at $\mathbf{r_d}$, and $\Phi_x\left(\mathbf{r},\mathbf{r_s},q\right)$ denotes the Laplace transformed exciting light density when the source at position $\mathbf{r_s}$ and the detection at $\mathbf{r}$。

The normalized Born-ratio model is introduced to eliminate the background difference. The detected flux is divided by the relevant excitation flux when the exciting source at position $\mathbf{r_s}$ and the detection at the position $\mathbf{r_d}$. It can be derived under the Robin boundary condition with the Fick's law[13]:

$$\Phi_m\left(\mathbf{r_s},\mathbf{r_d},q\right)=\frac{\Gamma_m^{(F)}\left(\mathbf{r_s},\mathbf{r_d},q\right)}{\Gamma_x^{(F)}\left(\mathbf{r_s},\mathbf{r_d},q\right)}\Phi_x\left(\mathbf{r_s},\mathbf{r_d},q\right)=\int_V cG\left(\mathbf{r_d},\mathbf{r},q\right)\Phi\left(\mathbf{r},\mathbf{r_s},q\right)x\left(\mathbf{r},q\right)dV \tag{1}$$

Here, $\Gamma_m^{(F)}(\mathbf{r_s},\mathbf{r_d},q), \Gamma_x^{(F)}(\mathbf{r_s},\mathbf{r_d},q)$ are the measured values of emission fluorescent light and exciting light for forward model, respectively.

To solve the unknown $x(\mathbf{r},q)$, the volume integral in Eq. (2) is discretized, where ΔV is referred to as the volume per unit cube. We have $x(\mathbf{r},q) \approx \sum_{n=1}^{N_{voxel}} x_n(q) u_n(\mathbf{r}) = x^T(q) u(\mathbf{r})$, where $u(\mathbf{r})$ is the unit position vector and $x(q) = \left[x_1(q), x_2(q) \ ;\cdots, x_{N_{voxel}}(q) \right]^T$. Eq. (2) can be translated into:

$$\Phi_m(q) = W(q) x(q) \tag{2}$$

For an infinite slab transmission model, the analytical solution of the diffuse equation under the extrapolated boundary conditions can be expressed as

$$\Phi(r_i) = \frac{c}{4\pi k} \sum_{m=-\infty}^{+\infty} \left\{ \frac{1}{\left| r_i - r^{+,m} \right|} \exp\left(-\mu_{eff}^e \left| r_i - r^{+,m} \right| \right) - \frac{1}{\left| r_i - r^{-,m} \right|} \exp\left(-\mu_{eff}^e \left| r_i - r^{-,m} \right| \right) \right\} \tag{3}$$

$$r^{\pm,m} = \left(x, y, z^{\pm,m} \right)$$

$$z^{+,m} = 2m(d + 2z_b) + z_0$$

$$z^{-,m} = 2m(d + 2z_b) - 2z_b - z_0$$

where $r^{\pm,m}$ present the locations of the symmetrical positive and negative sources according to the extrapolated boundary approximation. z_0 denotes the coordinate of the extrapolated boundary. The incident location of the single isotropic source is given by $z_0 = 1/\mu_s^{'}$, and the effective attenuation coefficient is $\mu_{eff}^e = \sqrt{3\mu_{ae}\mu_{se}^{'}}$.

The number of the fluorescence parameters is much greater than that of the measurement data due to the discrete process. Hence, the solution of the fluorescence parameters to the volume elements becomes an undetermined problem. Algebraic reconstruction technique based on the idea of solving linear equation is introduced to settle the problem above.

For the simultaneous solution of the fluorescence yield $\eta\mu_{af}(\mathbf{r})$ and fluorescence lifetime $\tau(\mathbf{r})$, a real transform factors is defined as $q_{1,2} = \mp 0.1Q$ and $q_{1,2} = \mp 0.5Q$, where $Q = 1 \Big/ \left[1 \Big/ \left(\mu_{ax}^{(B)} c \right) + 1 \Big/ \left(\mu_{am}^{(B)} c \right) + \tau^{(B)} \right]$ [14]. The fluorescence parameters can be obtained from Eq. (5)[15]:

$$\begin{cases} \eta\mu_{af}(\mathbf{r}) = (q_1 - q_2)x(\mathbf{r}, q_1)x(\mathbf{r}, q2) / \left[q_1 x(\mathbf{r}, q_1) - q2x(\mathbf{r}, q_2)\right] \\ \tau(\mathbf{r}) = -\left[x(\mathbf{r}, q_1) - x(\mathbf{r}, q_2)\right] / \left[q_1 x(\mathbf{r}, q_1) - q_2 x(\mathbf{r}, q_2)\right] \end{cases} \tag{4}$$

4. PHANTOM EXPERIMENTS

In order to verify the system and the reconstruction algorithm, experiments are implemented using solid phantoms instead of the breast cavity.

4.1 Phantoms and Measurement Condition

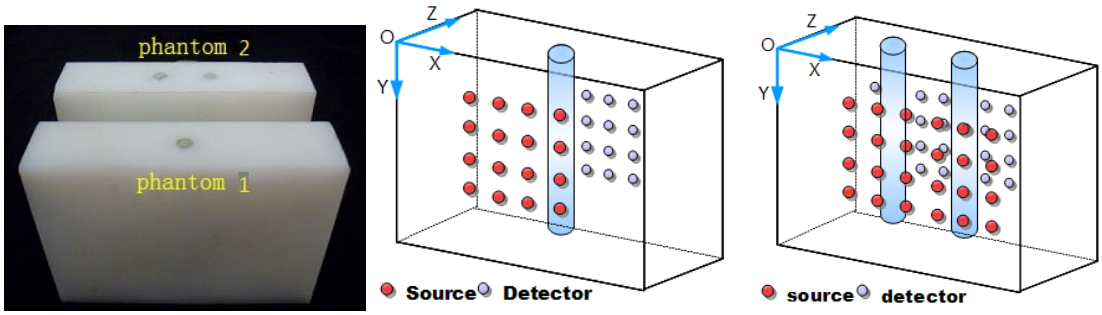

(a) (b) (c)

Figure 3 Photo and schematic diagram of phantoms

Two phantoms with the shape of 100mm×25mm×70mm are designed in this experiment and their photos are given in Fig. 3(a). The absorption coefficient and the scattering coefficient of the phantom background are similar to those of the breast tissue with μ_a =0.0038mm^{-1} and μ_s'=0.978mm^{-1}.

As shown in Fig. 3(b) and (c), the first phantom contains one fluorescent target in the center and the second phantom contains two fluorescent cylindrical targets with center-to-center separation of 20mm and diameter of 5mm, height of 60mm, respectively. The mixture of 1% intralipid solution and ICG fluorescence dye are filled in the cylindrical holes as the fluorescent targets with μ_a =0.0017mm^{-1} and μ_s'=0.87mm^{-1}.

As shown in Fig. 3(b), the scanning points for the single target phantom are arranged in a 4×4 grid with a 7mm center-to-center separation both on the source side and the detection side. The size of the canning area is thus 21mm×21mm. Likewise in Fig. 3(c), for the double targets phantom, the scanning points are arranged in a 6×4 rectangular grid and the size of the scanning area is 35mm×21mm. While one source illuminates the phantom, diffuse light emitted from the phantom surface are detected by all the detection points. Finally, total 256 data sets are measured for the single target phantom and 576 data sets for the double targets phantom, respectively.

4.2 Experiment Results and Analysis

Figure 4 illuminates the reconstructed results on the x-y, x-z, y-z plane of the single target phantom, where the dotted line marks the real location of the target. According to the tomography images of fluorescence yield (Fig. 4(a)) and lifetime (Fig. 4(b)) on x-y plane at z=15mm, it's obvious that fluorescence yield can be well reconstructed with the shape, location and size of the reconstructed target corresponding to the real one. Meanwhile, the location of the target shown in

the fluorescence lifetime image agrees well with the real object. The reconstructed lifetime is 500ps, which is almost identical to the actual fluorescence lifetime 560ps. Fig. 4(c) and Fig. 4(d) present the x-z plane tomography images of fluorescence yield and lifetime at y=30mm, respectively. While Fig. 4(e) and Fig. 4(f) show the y-z plane tomography images of fluorescence yield and lifetime at x=30mm, respectively. Compared with the reconstructed results on x-z plane and y-z plane, the quality of image in x-y profit is greater due to the insufficient of longitudinal data in the slab transmission model measurement.

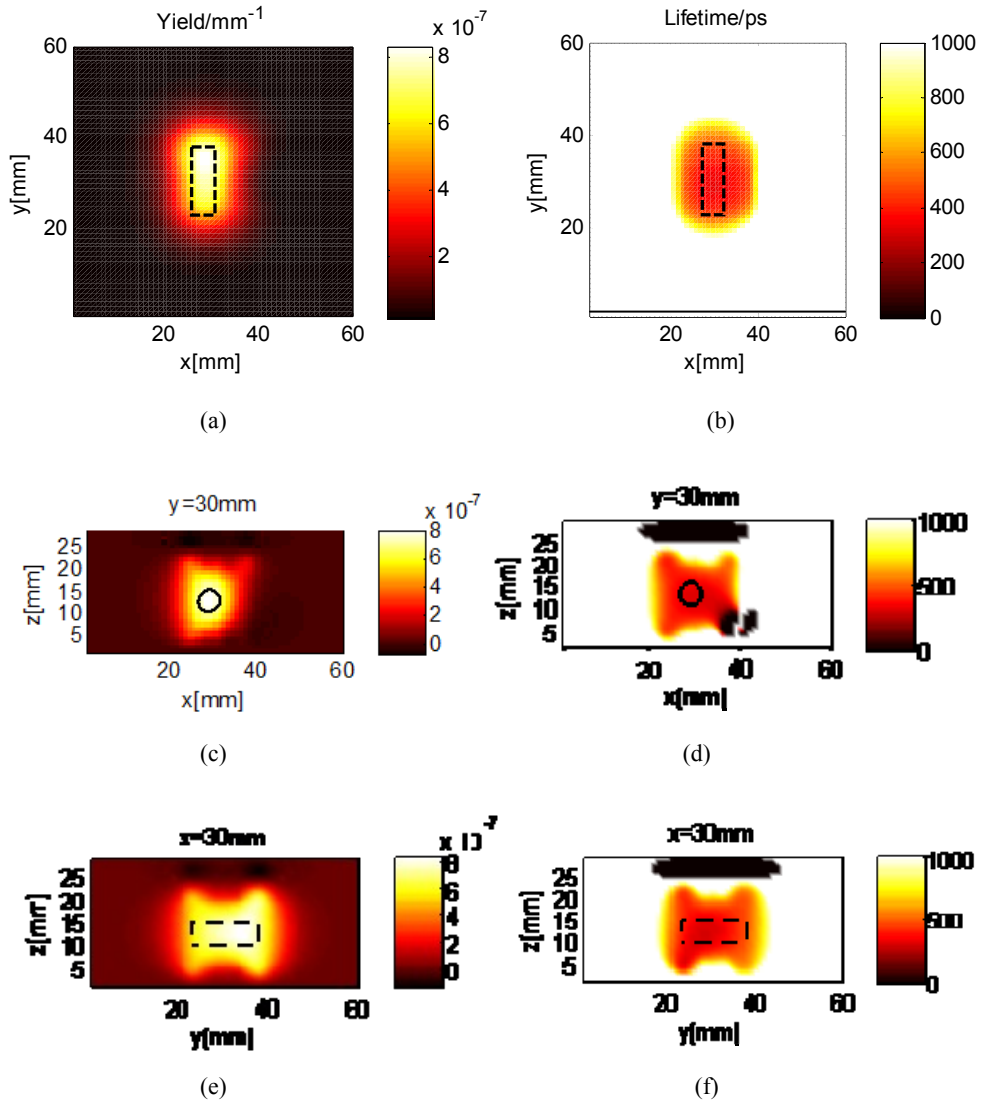

(a) (b)

(c) (d)

(e) (f)

Figure 4 Reconstructed results of the solid phantom with single fluorescent target

The reconstructed results of the double targets phantom are depicted in Fig. 5. Fig. 5(a) shows the reconstructed yield image on the x-y plane of the two targets when the fluorescence dye concentration ratio is 1:1. Though the volume of the reconstructed object is expanded and the boundary is fuzzy, the shape and location are consistent with those of the actual target. The two fluorescent targets can be better resolved when those edges separation is 15mm. The reconstruction value of fluorescence yield at y=30mm along the x axis is compared with the ideal value in Fig. 5(b). The

fluorescence yield reconstruction peak value ratio of the two fluorescent targets is 0.82:1, which is close to the ideal value of 1:1.

Figure 5(c) shows the fluorescence yield reconstruction image on the x-y plane of two fluorescent targets when the fluorescence dye concentration ratio is 1:2. The fluorescence yield reconstruction results demonstrate that the two fluorescent targets with different fluorescence dye concentration can be clear distinguished. The fluorescence yield reconstruction peak value ratio 1:1.826 of the two fluorescent targets is close to the ideal ratio 1:2 as depicted in Fig. 5(d). The experiment has proved that the reconstructed fluorescence yields are linear to the concentration of the fluorescence dye.

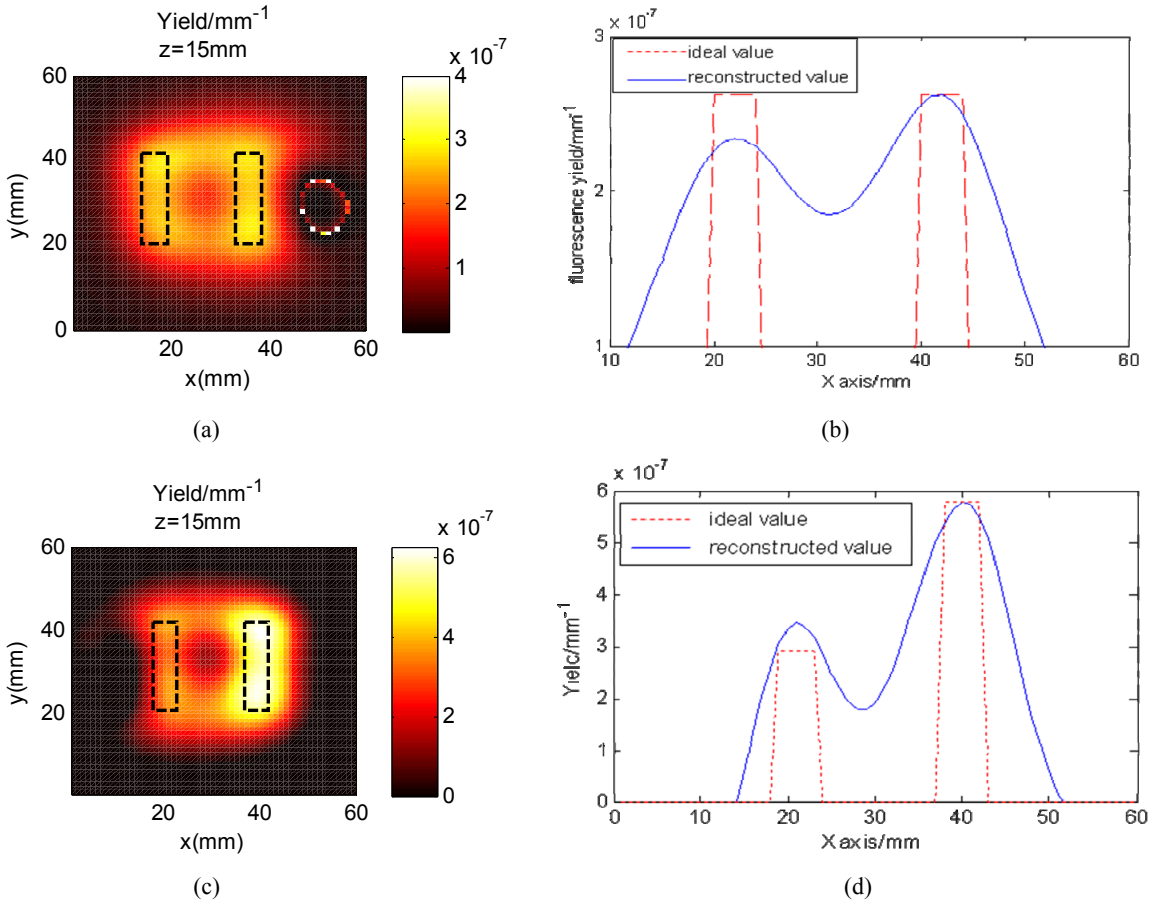

Figure 5 The reconstructed results of the double targets phantom with center to center separation of 20mm. (a) and (b) show the results when the contrast of the two fluorescent targets is 1:1; (c) and (d) show the results when the contrast is 1:2; (a) and (c) are the profiles of the reconstructed yield at z=15mm while (b) and (d) are the profiles of the reconstructed yield along the x axis at y=30mm.

5. CONCLUSION

A noncontact fluorescence tomography system for in-vivo breast tumor diagnosis was developed in this paper. The single source and detector structure not only eliminates the matching issues possibly exiting between the channels but also simplifies the system and reduces the cost. The time domain system based on time correlated photon counting technique can reconstruct the fluorescence yield and lifetime simultaneously with high sensitivity. The experiments results show

that the yield and lifetime of single fluorescent target can be well reconstructed through the developed measuring system and algorithm. When the phantom has double fluorescent targets with the center-to-center separation of 20mm and the edge separation of 15mm, the fluorescent targets can be differentiated from the yield image. Quantitative experiments show that the results achieve a good linearity to the concentration of fluorescent. The system can be further developed to be applied in clinical breast imaging.

ACKNOWLEDGEMENTS

The authors acknowledge the funding supports from the National Natural Science Foundation of China (30870657, 30970775), Chinese National Programs for High Technology Research and Development (2009AA02Z413) and Tianjin Municipal Government of China (09JCZDJC18200, 10JCZDJC17300).

REFERENCES

[1] Choe, R., Corlu, A., Lee ,K., "Diffuse optical tomography of breast cancer during neoadjuvant chemotherapy:A case study with comparison to MRI," Medical Physics 32(4), 128-131(2005).

[2] Dawei, D., Liu, F., Cao, J., "Synthesis and tumor targeting research of two near-infrared fluorescence probes," Chinese J. Lasers 37(11), 2735-2742(2010).

[3] Balas, C., "Review of biomedical optical imaging-a powerful, non-invasive, non-ionizing technology for improving in vivo diagnosis," Meas.Sci.Technol 20, 3-4(2009).

[4] Gibson, A. P., Hebden, J. C., Arridge, S. R., "Recent advances in diffuse optical imaging," Physics in Medicine and Biology 50, R3-R8(2005).

[5] Soloviev, V. Y., Tahir, K., Mcginty, J., Elson, D. S., Neil, M. A. A., French, P. M. W., Arridge, S. R., "Fluorescence lifetime imaging by using time-gated data acquisition," Appl. Opt. 46, 7384-7391(2007).

[6] Becker, W., Qu, J., Gao, F., [Advanced Time-Correlated Single Photon Counting Techniques], Science Press, Beijing, 3-8(2009).

[7] Schulz, R. B., Peter, J., Semmler, W., "Comparison of noncontact and fiber-based fluorescence-mediated tomography," Optics Letters 31(6),769-771(2006).

[8] Gao, F., Zhao, H., Yamada, Y., "Improvement of image quality in diffuse optical tomography by use of full time-resolved data," Appl. Opt. 41, 778-791(2002).

[9] Zhang, L., Gao, F., Li, J., "Reconstructing three-dimensional fluorescent parameters using time-resolved data based on transmittance and reflection measurements," Chinese J. Lasers 36(10), 2552-2556(2009).

[10] Zhang, L., Gao, F., Li, J., Zhao, H., "Reconstruction fluorescent parameters using time-resolved data based on experimental measurement," Proc. SPIE 7557, 1-7(2010).

[11] Li, J., Gao, F., Yi, X., Zhang, L., Zhao, H., "An Methodological and Experimental Investigation on Time-Domain Diffuse Fluorescence Tomography of Analytic Based on Two-Dimensional Circular Scheme," Chinese J. Lasers 37(11), 2743-2748(2010).

[12] Gao, F., Zhao, H., Tanikawa, Y., and Yamada Y., "A linear, featured-data scheme for image reconstruction in time-domain fluorescence molecular tomography," Opt. Express 14(16), 7109-7124(2006).

[13] Gao, F., Zhao, H., Zhang, L., Tanikawa Y., Marjono, A., Yamada, Y., "A self-normalized, full time-resolved method of fluorescence diffuse optical tomography," Opt. Express 16(17), 13104-13121(2008).
[14] Gao, F., Li, J., Zhang, L., Poulet, P., Zhao, H., and Yamada, Y., "Simultaneous fluorescence yield and lifetime tomography from time-resolved transmittances of small-animal-sized phantom," App. Opt. 49(16), 3163-3172(2010).
[15] Gao, F., Li, J., Zhang, L., Zhao, H., "A Methodological and Experimental Investigation on Time-Domain Fluorescence Diffuse Optical Tomography Based on Analytic Transmission Scheme," Journal of Tianjin University 43(6), 557-561(2010).